



PERGAMON



Atmospheric Environment 34 (2000) 195–205

**ATMOSPHERIC
ENVIRONMENT**www.elsevier.com/locate/atmosenv

Seasonal variability of ozone dry deposition under southern European climate conditions, in Portugal

C.A. Pio^{a,*}, M.S. Feliciano^a, A.T. Vermeulen^b, E.C. Sousa^a^a*Departamento de Ambiente e Ordenamento, Universidade de Aveiro, Campus de Santiago, 3800 Aveiro, Portugal*^b*Energy Research Foundation, PO Box 1, 1755 ZG Petten, Netherlands*

Received 12 January 1999; accepted 18 May 1999

Abstract

Ozone dry deposition measurements were carried out during approximately one year over a flat grass field in Portugal. The results show prominent diurnal and seasonal patterns in deposition flux, dry deposition velocity and surface resistance, especially for the daytime period. Dry deposition velocities vary diurnally from a minimum of 0.1 cm s^{-1} , during the night to a maximum of $0.2\text{--}0.5 \text{ cm s}^{-1}$ during the day. The observed canopy resistance (R_c) varies from values higher than 500 s m^{-1} , at night, to a minimum of 200 s m^{-1} , around noon. Seasonal variation is characterised by daytime R_c values much larger in summer than in winter and spring, while nighttime values do not show any evident seasonal pattern. This behaviour can be ascribed to the stomatal intake, which represents the most important controlling factor on ozone dry deposition. The Wesely parameterisation scheme of surface resistance predicts R_c diurnal cycles reasonably well. However, the observed canopy resistance seasonal cycle is completely different from Wesely predictions, since season parameters in Wesely's parameterisation were defined for a vegetation growing cycle different from that prevailing in our conditions. © 1999 Elsevier Science Ltd. All rights reserved.

Keywords: Ozone dry deposition; Surface resistance; Stomatal resistance; Diurnal variation and parameterisation

1. Introduction

Ozone is an important atmospheric pollutant that intervenes on tropospheric chemistry and global climate, also affecting the health of animals and plants (Jacobson and Hill, 1970; Treshow and Anderson, 1989). For a correct application of abatement strategies, for ozone and its precursors, it is important to understand the factors that control atmospheric ozone levels, namely the removal by dry deposition processes (Fehsenfeld and Liu, 1993; Pederson et al., 1995).

A large number of field studies have been performed in the past concerning the dry deposition of ozone, principally in the United States and northern European regions (O'Dell et al., 1977; Wesely et al., 1978; Leuning et al., 1979; Galbally and Roy, 1980; Delany et al., 1986; Padro et al., 1991; van Pul, 1992). These experimental

data have served as a basis for the development of parameterisation schemes used in atmospheric models to describe ozone dry deposition mechanisms.

To be completely acceptable, deposition algorithms developed on the basis of experimental data from northern latitudes need to be tested under environmental conditions prevailing in South Europe. South European regions have weather and vegetation growing cycles different from northern latitudes. In the south, winters are mild and summers are hot and dry. Moreover, vegetation grows in winter and spring periods, drying and dying during summer.

In the framework of the European Union environmental research program, integrated in the SREMP project (Surface Resistance Emergency Measurement Program), a field experiment was carried out during several seasons, over a grassland in the Aveiro region (Portugal) with the purpose of filling existent gaps concerning ozone dry deposition in South European conditions. In this paper our attention will be focused on the

* Corresponding author.

E-mail address: casimiro@dao.ua.pt (C.A. Pio)

analysis of the temporal variability of ozone dry deposition and on the evaluation of a single-layer canopy resistance model based on Wesely formulation (Wesely, 1989), which was developed to describe ozone deposition in the Eastern United States.

2. Dry deposition modelling

The dry deposition flux, F , of an air pollutant has frequently been defined as the product of the ambient concentration, C , and the deposition velocity, V_d :

$$F = -V_d * C \quad (1)$$

Dry deposition is usually described by drawing with Ohm's law analogy, i.e., by considering the existence of several resistances to the pollutant transference from the atmosphere to the deposition surface (Garland, 1977; Wesely and Hicks, 1977; Fowler, 1978; Baldocchi et al., 1987). V_d is defined as the reciprocal of the sum of three resistances in series (aerodynamic resistance, R_a , quasi-laminar boundary layer resistance R_b and surface or canopy resistance, R_c):

$$V_d = \frac{1}{R_a + R_b + R_c} \quad (2)$$

By computing V_d , R_a and R_b , directly from micro-meteorological measurements (Hicks et al., 1987; Erisman et al., 1994a), the overall canopy resistance, R_c , can be derived from Eq. (2). Then, time series of calculated R_c values could be used to obtain a canopy resistance parameterisation or to validate model results.

Canopy resistance, R_c , is often the controlling resistance of deposition flux and, therefore, considerable effort has been devoted in the development of better parameterisations for incorporation in deposition models. The analytical description of R_c has been difficult since it involves physical, chemical and biological inter-action of the pollutant with the deposition surface.

Several models of different complexity have been developed to represent the dry deposition on vegetation covered surfaces (Baldocchi et al., 1987; Baldocchi, 1988; Wesely, 1989; Padro et al., 1991, 1992). Dry deposition models have to be as simple and generalised as possible for an easier application in atmospheric modelling. Models based on the big-leaf approach are therefore most widely used (Hicks and Matt, 1988). In these models, a single stomata resistance, a single mesophyll resistance and a single cuticular resistance are used to characterise the canopy as a whole.

Frequently R_c parameterisation can be simplified and reduced to the sum of two resistances in parallel, the stomatal resistance, R_{stom} , associated to diffusion through the stomata, and the non-stomatal resistance, R_{nstom} , that includes transference to the vegetation cuticle and the

uncovered soil surface:

$$R_c = \frac{R_{\text{stom}} R_{\text{nstom}}}{R_{\text{stom}} + R_{\text{nstom}}} \quad (3)$$

From the Baldocchi model (Baldocchi et al., 1987), which derives bulk stomatal resistance from the specific characteristics of individual leaves and light penetration in the canopy, the stomatal conductance for a specific pollutant ($g_{\text{stom}} = 1/R_{\text{stom}}$) can be scaled up from leaf to canopy level with the equation:

$$g_{\text{stom}} = \sum_{i=1}^n \{ [\text{LAI}_{\text{sun},i} g_{\text{stom},i} (\text{PAR}_{\text{sun}}) + \text{LAI}_{\text{shade},i} g_{\text{stom},i} (\text{PAR}_{\text{shade}})] f_{1,i} (W_D) f_{2,i}(T) \} \frac{D_{\text{H}_2\text{O}}}{D}, \quad (4)$$

where n represents the number of vegetation species, LAI_{sun} is the sunlit leaf area index, $\text{LAI}_{\text{shade}}$ the shaded leaf area index, PAR_{sun} and $\text{PAR}_{\text{shade}}$ are the flux densities of photosynthetically active radiation (PAR) on sunlit and shaded leaves, and $D_{\text{H}_2\text{O}}$ and D the diffusion coefficients of water vapour and the pollutant in the air.

The functions g_s , f_1 , and f_2 relate leaf stomatal conductance for water vapour and for each vegetation species, $g_{\text{stom},i}$ with, PAR, air temperature, T , and vapour deficit pressure, W_D , respectively:

$$g_{\text{stom},i} = [g_{s,i}(\text{PAR})][f_{1,i}(W_D)][f_{2,i}(T)] = \left[\frac{\text{PAR}}{r_{\text{smin},i} (b_{rs,i} + \text{PAR})} \right] [1 - b_{v,i} W_D] \left[\frac{T}{30} \left(\frac{40 - T}{10} \right)^{0.25} \right], \quad (5)$$

where r_{smin} , b_{rs} and b_v are parameters defined for each i vegetation species.

Detailed models such as the Baldocchi parameterisation allow better insight in dry deposition mechanisms, but the large amount of information required limit their usefulness to application in transport modelling.

The uptake by stomata in the whole canopy may be described in a simpler formulation, only as a function of global radiation intensity (G) and ambient temperature (T) (Wesely, 1989):

$$R_{\text{stom}} = r_i \left\{ 1 + \left[\frac{200}{G + 0.1} \right]^2 \right\} \left\{ \frac{400}{T(40 - T)} \right\} \frac{D_{\text{H}_2\text{O}}}{D} + R_m \quad (6)$$

where r_i is the minimum bulk canopy stomatal resistance for water vapour, and R_m is the mesophyll resistance. R_m is frequently disregarded for pollutants such as ozone because of the high reactivity of the pollutant with the mesophyll (Rich et al., 1970; Leuning et al., 1979; Wesely, 1989).

3. Experimental details

A measuring station was mounted, between November 1994 and October 1995, in the Northwest side of a 40 ha flat area, providing a reasonable fetch for almost all directions. The study area, called “Polder Piloto de Sarrazola”, is located 9 km inland from the western coast of Portugal (40°42'20"N/8°37'15"W). The surface is a fertile area with permanent and temporary meadows for grazing and hay growth. Normally, the vegetation starts to grow in early autumn, reaching its maximum activity at late winter or spring. In late July and August the grass was almost completely dry.

During the field campaign, vegetation height, distribution of species, leaf area index (LAI) and biomass density were measured and calculated. Three species are predominant, with a relative abundance that varies with the season of the year (10–65% *Festuca arundinaceae*; 30–50% *Trifolium repens*; 1–13% *Plantago lanceolata*). Vegetation height varied between a minimum of 10 cm in November to a maximum of 70–80 cm in mid spring, with a total LAI ranging between 2.5 and 4.5, during the same period.

A fully automatic system, developed by the Netherlands Energy Research Foundation (ECN), was used for continuous eddy correlation measurements of momentum, sensible heat and ozone surface fluxes. The system consists fundamentally of a 3D ultra-sonic anemometer (Solent Research Gill) coupled with a fast response ozone sensor – GFAS/OS-G-2 – (Güsten et al., 1992; Güsten and Heinrich, 1996a), mounted vertically on the top of a 5 m mast. Ozone fluxes were obtained by correlating the measured vertical wind velocity with ozone fluctuations ($F = \overline{w'c'}$) (Baldochi et al., 1988; Businger, 1989). A slow response ozone analyser (Thermo-Electron model 49) permitted the continuous on-line calibration of the GFAS/OS-G-2 sensor.

Total solar radiation received at the earth's surface was measured using a Casella Solarimeter. Temperature and relative humidity were monitored with a Rotronic MP300 probe at a height of 3 m above the surface.

Eddy correlation measurements were acquired and processed in real time according to the algorithm imple-

mented by McMillen (McMillen, 1986, 1988; Baldochi et al., 1988; Güsten and Heinrich, 1996a). In short, analog signals from eddy measurements were detrended with a 200 s high-pass digital recursive filter. Instrument delay time was determined by rerunning the software and calculating ozone fluxes for several lag times relative to wind measurements (Güsten et al., 1996b). Errors associated with the inappropriate orientation of the wind sensor and the presence of non-horizontal mean wind streamlines, were minimised by means of 3D co-ordinate rotation performed at the end of each measurement cycle period (Wesely, 1970).

Sensible heat flux (H) and turbulent parameters such as Monin–Obukhov Length (L) and friction velocity (u_*) were directly calculated from instantaneous eddy correlation data. Aerodynamic and quasi-laminar resistances were computed according to formulation presented in Erisman et al. (1994a):

$$R_a + R_b = \left\{ \frac{1}{ku_*} \left[\ln \left(\frac{z-d}{z_0} \right) - \Psi_h \left(\frac{z-d}{L} \right) + \Psi_h \left(\frac{z_0}{L} \right) \right] \right\} + \left\{ \frac{2}{ku_*} (Sc/Pr)^{2/3} \right\}, \quad (7)$$

where k is the von Karman constant ($= 0.4$), d is the displacement length, z_0 is the roughness height and $\Psi_H(z/L)$ is the integrated stability correction function for heat. Pr and Sc are Prandtl and Schmidt numbers, respectively. Canopy resistance (R_c) was estimated from eddy correlation measurements as the residual of the total resistance by using Eqs. (1) and (2).

Leaf stomatal conductance and net photosynthesis rates of the predominant species were measured intermittently in the field and laboratory with a portable photosynthesis system (Licor LI-6400).

4. Experimental results and discussion

A total of 17,500 measuring periods (15 min averaged) were recorded during the experiment. Using a set of restrictive criteria (Garrat, 1980; Erisman et al., 1994b), periods with unfavourable conditions for a correct flux calculation were removed from the data set (see Table 1).

Table 1
Selection criteria applied to the 15 min time series of ozone data

% of Remaining data Criteria	February	March	April	May	June	July	August	September	Total average
$U > 1 \text{ m s}^{-1}$	91.7	83.9	80.6	90.2	81.6	86.8	78.1	77.6	83.8
$U > 0.05 \text{ m s}^{-1}$	84.6	71.6	63.5	82.6	73.1	78.1	67.9	67.8	73.7
$ L > 1 \text{ m}$	84.3	70.9	62.2	81.8	71.8	77.3	66.6	66.8	72.7
$\text{O}_3 \text{ Flux} < 0 \mu\text{g m}^{-2} \text{ s}^{-1}$	82.4	69.4	59.2	81.2	71.3	69.5	65.2	65.7	70.5
Initial points	1607	2091	1612	2580	2177	2318	2715	2341	17441

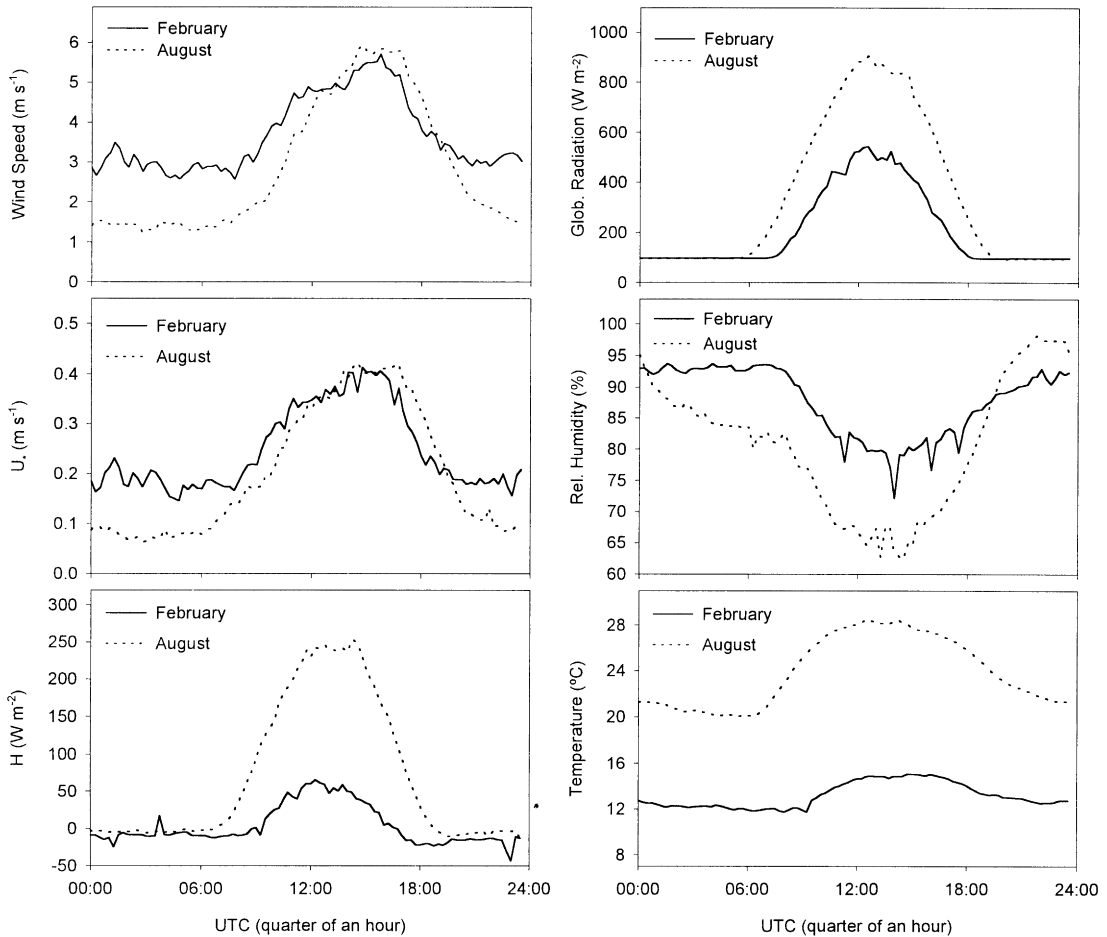


Fig. 1. Diurnal variation of wind velocity u , friction velocity u_* , sensible heat H , temperature T , relative humidity RH , and global radiation G , obtained from the quarter of an hour measurements, for February and August.

As most of the removed periods are associated with low flux conditions, the filtered data set lead to some overestimation of average flux and deposition velocity for ozone, principally during nighttime periods.

Fig. 1 shows the average diurnal variation of the wind velocity (u), friction velocity (u_*), temperature (T), global radiation (G), relative humidity (RH), and heat flux (H), calculated for two representative months, February and August. The wind speed starts rising in the early morning, reaching maximum values of approximately 6 m s^{-1} in mid afternoon, and then decreasing to less than 3 m s^{-1} at night. During the daytime, the wind blows predominantly from the Northwest sector, while for the night periods the predominant sector is from Southeast. Temperature follows the usual diurnal and seasonal trend. Inversely, the relative humidity reaches values close to saturation at night, decreasing during the day to values around 70–80%. Turbulence generally decays rapidly after sunset as a consequence of surface cooling.

During summer and spring seasons a stable stratified boundary layer was frequently observed at night.

These diurnal variations of the micrometeorological parameters allow an evaluation of the prevailing weather conditions in the Aveiro region. Because of its proximity to the sea border, the local climate is strongly influenced by sea/land breezes with large diurnal cycles, especially in spring and summer.

During the sampling campaign, periods of rain occurred with more frequency between late autumn and early spring, with a total rainfall of approximately 500 mm. During summer rainfall events were limited only to a few days. However, even during periods without rainfall, water droplets were observed on the vegetation surface during late night and morning as a result of dew or fog deposition.

The temporal variability of ozone concentration (C), ozone flux (F), ozone deposition velocity (V_d), and ozone residual surface resistance (R_c), are summarised in Fig. 2.

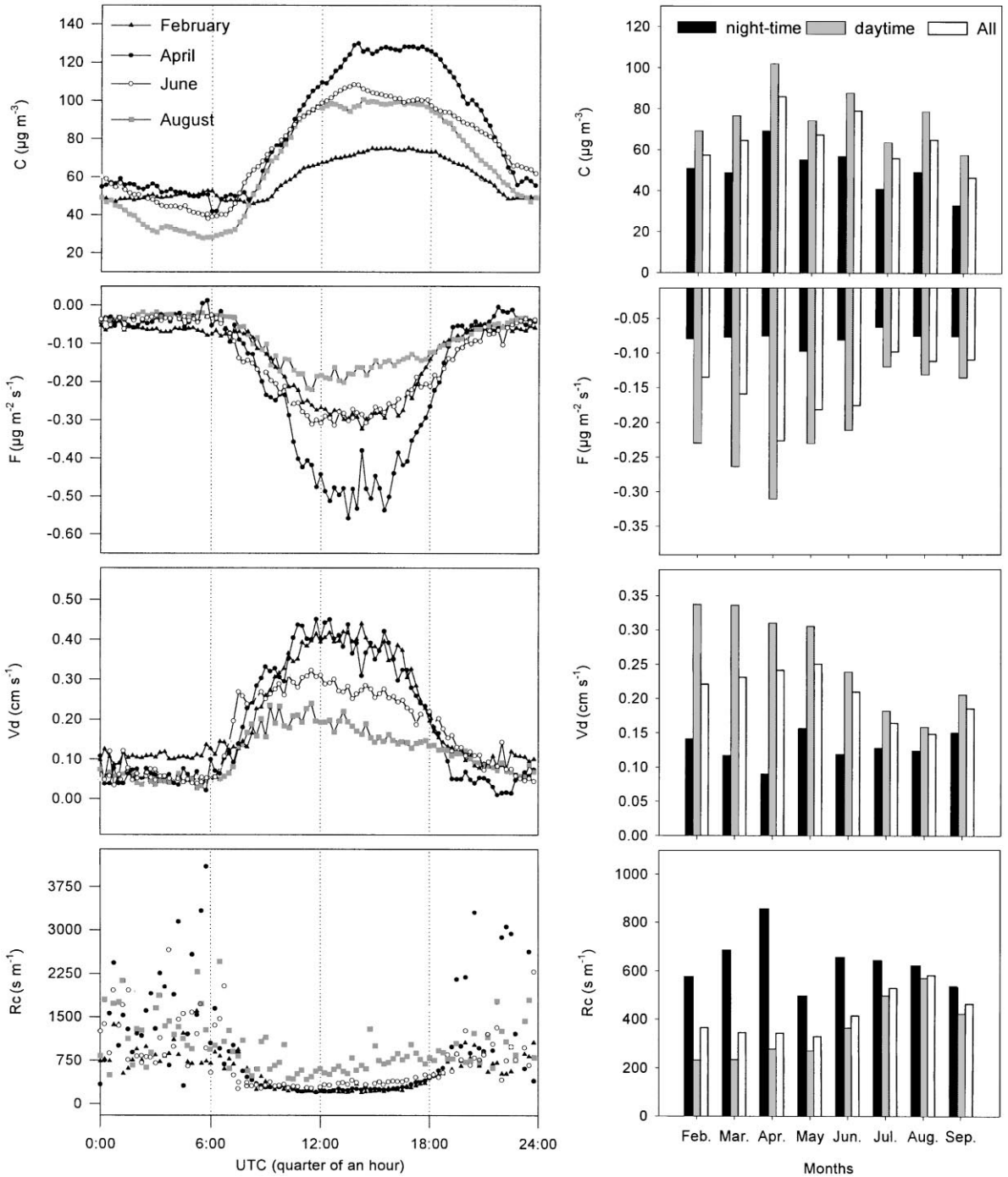


Fig. 2. (Left side). Averaged diurnal variation of concentration C , dry deposition flux F , dry deposition velocity V_d and surface resistance R_c , for February, April, June and August. The xx-axis represents the universal time (UTC: Universal Time Coordinate). The yy-axis represents the arithmetic average of all values available for each 15 min time interval for the whole month. (Right side): Monthly values of concentration C , dry deposition flux F , dry deposition velocity V_d and surface resistance R_c , given as median over all day, daytime and nighttime.

They are displayed as: (a) average diurnal variation obtained from the observed time series for February, April, June and August; and (b) monthly median values obtained for three different periods (*total*, *daytime* and *nighttime*). Daytime is defined here as the time period comprised between sunrise and sunset. With this type of analysis, local specific conditions are averaged out. Sporadic errors are filtered out as well. This analysis allows the establishment of general links between dry deposition parameters and weather or surface conditions, such as stomata opening.

Both Fig. 2a and 2b show a clear daily and seasonal pattern of ozone concentration and dry deposition parameters. One can also observe that during the whole sampling campaign deposition rates and deposition velocities are higher during the daytime and lower at night.

Ozone levels are highly variable showing a straight correlation with local meteorology. The pattern is characterised by daily maximum values (ranging from about $80 \mu\text{g m}^{-3}$ in February to $140 \mu\text{g m}^{-3}$ in April), occurring generally in the early afternoon. Around sunset, ozone concentrations start decreasing slowly, reaching minimum values (varying between 30 and $60 \mu\text{g m}^{-3}$) during early morning hours. Higher concentration values occur in spring/summer, with peak values measured in April. This temporal behaviour is a result of atmospheric processes including photochemical ozone production and turbulent downward mixing from the upper troposphere (Galbally et al., 1986; Warneck, 1988).

Ozone deposition fluxes follow a similar daily pattern, but with maximum and decreasing parts happening somewhat earlier in the day. The seasonal trend is characterised by maximum daytime fluxes occurring in mid spring (ca. $-0.5 \mu\text{g m}^{-2} \text{s}^{-1}$) and minimum daytime values in summer (around $-0.15 \mu\text{g m}^{-2} \text{s}^{-1}$). Although the maximum ozone deposition rates occur also in April, as for ozone concentration, the lowest values are observed in July and August.

As shown in Fig. 2, the dry deposition velocity showed minimum nighttime values lower than 0.1 cm s^{-1} and maximum midday values ranging from 0.2 cm s^{-1} , in August, to 0.5 cm s^{-1} , in February and April. This observed diurnal variation in dry deposition velocity has also been found in other ozone dry deposition studies over grass (Droppo, 1985; Delany et al., 1986; Padro et al., 1994b) and over other vegetation species (Wesely et al., 1982 (soybean); Padro, 1996 (cotton)). These authors found diurnal variations ranging between night-time values lower than 0.1 cm s^{-1} and midday values up to 1 cm s^{-1} . Cieslik and Labat (1997) found maximum daytime ozone deposition velocities of about 0.2 cm s^{-1} , over a 'Mediterranean pseudosteppe' ecosystem covered with low vegetation during the dry season.

The majority of the published studies are related to shorter measuring campaigns, which may not represent the wide range of the environmental conditions involved

in this study and, therefore, when this happens deposition values can be exceptionally higher or lower. At our site, the seasonal pattern of ozone dry deposition velocity was characterised by higher values in winter/spring than in summer, for daylight conditions. For the nighttime period, no clear and consistent variation in V_d was found.

The daily course of the canopy resistance R_c decreases from values higher than 600 s m^{-1} , soon after sunrise, to minimum midday values ranging between 200 s m^{-1} , in winter/spring, and 500 s m^{-1} , in summer. Around sunset R_c increases, reaching large and scattered values, which remain at this level throughout the night. This broad scatter can be explained, to a large extent, by the low signal-to-noise ratio of the equipment electronics signals.

Similar to the seasonal pattern observed for V_d , the seasonal pattern in the R_c is mainly observed for the daytime period. Daytime canopy resistance exhibits minimum values between February and May, starting to increase slightly from that time onwards. In July and August, the daytime canopy resistance rises considerably leading, hence, to the lower daytime/nighttime ratios.

Although diurnal variation of aerodynamic and quasi-laminar boundary layer resistances are not presented in this paper, it is possible to conclude that R_c is the major contributor and determines the shape of the diurnal course of total resistance since it is much higher than R_a and R_b , especially for daytime period. At night, R_c continues to have higher values than R_a and R_b , but under strong stable conditions (eliminated from analysis by the rejection criteria) the dry deposition velocity is also strongly limited by R_a , due to the low atmospheric turbulence.

The variability of canopy resistance can be interpreted as an effect of the vegetation stomatal activity. During the day, ozone molecules diffuse through the opened stomata and react rapidly inside the sub-stomatal cavity (Musselman and Massman, 1999). At night, stomata close and R_c increases significantly. Ozone dry deposition also follows the pattern of the vegetation growing cycle. The lowest R_c values are observed in winter and spring and coincide with the period of maximum physiological activity. In summer months, during which the predominant vegetation is biologically inactive, the ozone removal diminishes considerably.

Average and median diurnal cycles of ozone canopy resistance, calculated for each month (from February to September), were fitted with the Wesely resistance canopy model (Wesely, 1989; Wamsley and Wesely, 1996), through Eqs. (3) and (6). In these equations R_{nstom} and r_i were estimated by a non-linear optimisation procedure. The comparison for each month between median diurnal cycles and the respective modelled resistance values is given in Fig. 3. In a general way, the model compares well with the experimental data, especially during periods when ozone is transferred efficiently through the stomata, in the winter and spring months. The larger uncertainties

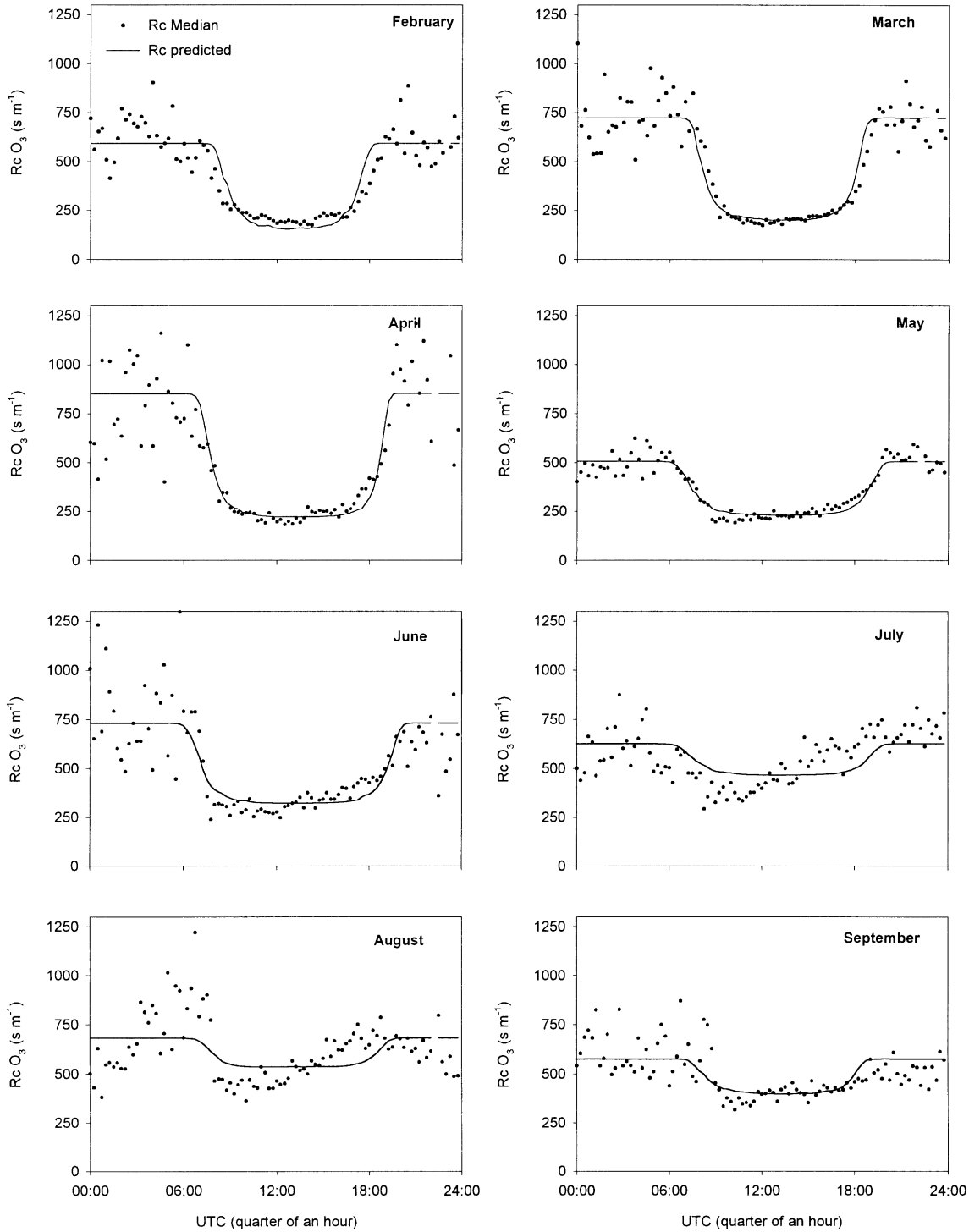


Fig. 3. Median diurnal curves of surface resistance calculated from the measurements and predicted by non-linear fitting of the Eqs. (3) and (6) to the experimental data.

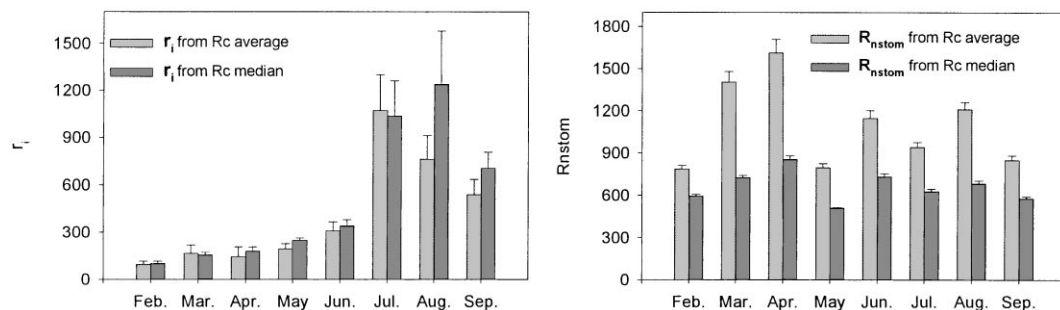


Fig. 4. Monthly variability of fitted r_i and R_{nstom} for ozone dry deposition, obtained from average and median diurnal R_c variation. Upper bars represent the respective standard errors.

associated with the daytime periods in summer, as a result of the significant reduction of fluxes, lead to a lower agreement. The agreement between predicted and measured values is quite reasonable again for September.

The fitted parameters (r_i and R_{nstom}) are displayed in Fig. 4, for both R_c arithmetic mean and R_c median diurnal cycles, although we believe that median is a more suitable parameter for measuring the central tendency of this type of data. It is important to note that the parameterisation scheme assumes no diurnal variations of R_{nstom} , whose magnitude is determined, to a large extent, by the nighttime R_c values. Nighttime R_c values have also some influence on the predicted r_i ; higher R_{nstom} lead to slight underestimates of r_i and, lower values of R_{nstom} result in a small overestimate of r_i . However, this simplification does not lead to serious errors since the non-stomatal resistance to ozone generally is quite large and diurnal variation of R_{nstom} seems irrelevant when R_{stom} is much lower than R_{nstom} .

From Fig. 4 it is possible to conclude that r_i follows the vegetation growing cycle with maximum values during the August. The r_i values tabulated by Wesely (1989) and Walmsley et al. (1996) for this type of surface coverage seem to be correct if the different effects of the seasons in the vegetation growing cycle are taken into account. In Aveiro and also in other regions in Southern Europe the vegetation growing cycle is quite different from that observed in more temperate regions; the vegetation is more active during the mild winter and spring and dies during the hot dry summer.

R_{nstom} represents the resistance to ozone deposition over the cuticle of active vegetation, surface of dead plant material and underlying soil (Galbally and Roy, 1980). From observations, it is possible to conclude that these non-stomatal sinks exhibit a limited efficiency in the ozone removal at our site.

As shown in Fig. 4, the calculated median values of R_{nstom} do not reveal any detectable seasonal trend and remain approximately constant along the various months

of the year. There is still some uncertainty about the processes and reactions involving the deposition over the external surface of vegetation and bare ground. Normally it would be expected that vegetation surfaces wetted by rain, fog or dew, would pose a larger resistance to ozone deposition, because of the low solubility of the pollutant in water. Therefore, at our site, we would expect to have a decrease in R_{nstom} from winter months, when the vegetation is more frequently wet, to the summer dryer months. We analysed in detail our data for trends but no strong correlation could be found between nocturnal R_c and rainfall events or relative humidity. So it seems that, either the wetness of vegetation has no effect on the resistance to ozone deposition on the vegetation cuticle, or there are opposite compensating effects that maintain the overall R_{nstom} approximately constant along the various seasons. One of these effects is for example the senescence of the vegetation in summer. Massman (1993) pointed out that dead vegetation has a low contribution to ozone removal but it has not been demonstrated yet if dead vegetation surface is less or more reactive towards ozone than the surface of active vegetation.

Several studies demonstrated that wetted surfaces may be an effective sink for ozone, possibly as a result of the chemical interaction of ozone with reactive chemical compounds dissolved in water layers (Wesely, 1989; Fuentes et al., 1994; Padro et al., 1994a; Stocker et al., 1995).

Our ignorance about R_{nstom} controlling factors has limited the evaluation of the magnitude of non-stomatal sinks relative to the amount of ozone lost through vegetation stomata, since the night values may not be representative of the daytime non-stomatal processes. Güsten et al. (1996b) found a daily pattern in the ozone R_c values over sandy soil in the Libyan desert, with values ranging from $\approx 800 \text{ s m}^{-1}$ during day to $\approx 4000 \text{ s m}^{-1}$ at night. The authors attributed this daily variation to changes in the humidity of sand particles. In spite of the evident daytime/nighttime variation both values seem very high when compared with values obtained over vegetative

surfaces. Temperature and solar radiation have also been pointed out as potential factors that enhance the destruction of ozone over external surfaces (Galbally and Roy, 1980; Coe et al., 1995).

As a test to the correctness of the Wesely dry deposition model results derived from our data, the single leaf stomatal resistances for water vapour measured for each vegetation species with the portable photosynthesis system Licor Li-6400 (see Fig. 5) were used, together with information on biomass distribution, for an independent calculation of the canopy stomatal resistance.

This calculation was made by first adjusting leaf stomatal conductances measured for each vegetation species to Eq. (5), determining $r_{smin,i}$, $b_{rs,i}$ and $b_{v,i}$. Then, employing measured data of PAR, air temperature, vapour deficit pressure and green leaf area index, canopy stomatal resistance was estimated for every 15 min periods, by using Eq. (4). Finally, median daytime variation of stomatal resistance was calculated from previous 15 min averages, for each month.

Fig. 6 shows, as an example, the median values for ozone stomatal resistance variation along the day in March, calculated by the Baldocchi model (Eqs. (4) and (5)) from individual leaf measurements and by the Wesely model (Eq. (6)) using r_i derived from the eddy correlation data. The two methodologies produce similar values for the stomatal resistance, although the values calculated from the Wesely model are higher than the calculations resulting from the Baldocchi model. Seeing that the imprecision of the biomass distribution (Nobel, 1991), hinders an accurate estimation of the canopy stomatal resistance by using Eq. (4), the differences are within the expected errors for each model.

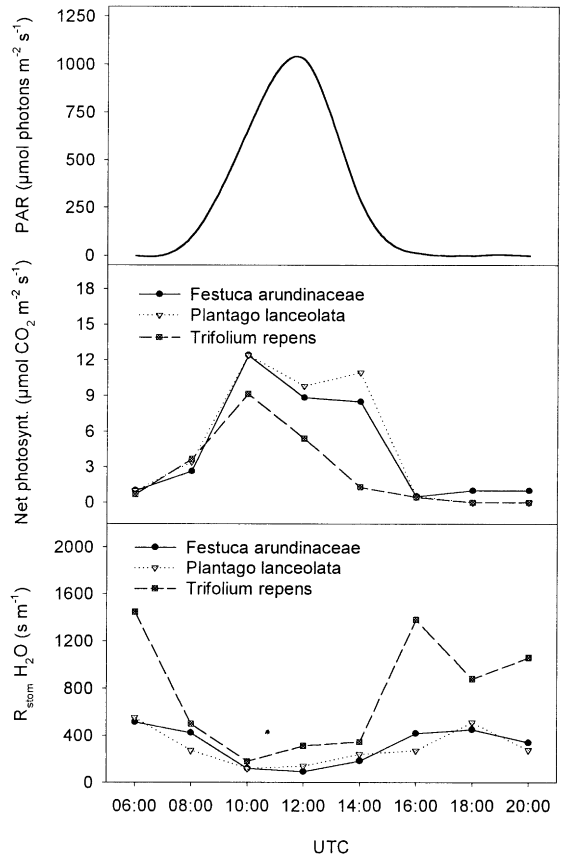


Fig. 5. Photosynthetic active radiation (PAR), leaf photosynthesis rates and leaf stomatal resistances plotted for the three dominant vegetative species in the sampling site.

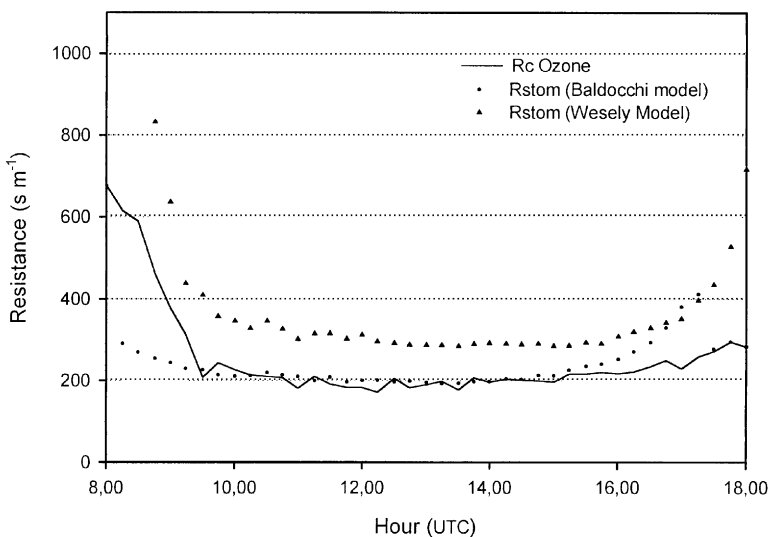


Fig. 6. Comparison between average daytime variation of ozone surface resistance obtained from eddy correlation measurements and bulk ozone stomatal resistance computed from Eqs. (5) and (6), for March 1995.

5. Conclusions

Measurements of ozone fluxes were carried out during eight consecutive months. Basic rejection criteria were applied in order to assure high-quality results. Application of these criteria resulted in the elimination of about 30% of the original data. The remaining data set provided a reasonable coverage of the temporal variability of deposition parameters and allowed to assess the applicability of a parameterisation scheme developed to describe this phenomenon.

The temporal R_c variability was interpreted as a function of the vegetation stomatal activity. Ozone dry deposition rates at night are much lower than daytime values. No evidence was found on the influence of other factors, such as surface wetness, surface temperature, etc., in ozone destruction at the deposition surfaces.

An algorithm based on the Wesely model was reasonably well adjusted to ozone R_c values derived from eddy correlation measurements. From the obtained results, it is possible to conclude that the simple Wesely model is able to describe the ozone dry deposition in this southern European ecosystem with reasonable accuracy, if the model parameters are adapted to take into account the vegetation seasonal growing cycle.

Acknowledgements

We gratefully acknowledge the European Commission and the Junta Nacional de Investigação Científica, for financial support through the projects EV5V-CT93-316 and PRAXIS/3/3.2/AMB/38/94, respectively. We also wish to thank the *Instituto de Estruturas Agrárias e Desenvolvimento Rural* who permitted the measurements at the “Polder Piloto” of Sarrazola and all research groups who participated in the SREMP Project.

References

- Baldocchi, D.D., Hicks, B.B., Camara, P., 1987. A canopy resistance model for gaseous deposition to vegetated surfaces. *Atmospheric Environment* 21, 91–101.
- Baldocchi, D.D., 1988. A multi-layer model for estimating sulfur dioxide deposition to deciduous oak forest canopy. *Atmospheric Environment* 22, 869–1101.
- Baldocchi, D.D., Hicks, B.B., Meyers, T.P., 1988. Measuring biosphere-atmosphere exchanges of biologically related gases with micrometeorological methods. *Ecology* 69, 1331–1340.
- Businger, J.A., 1986. Evaluation of the accuracy with which dry deposition can be measured with current micrometeorological techniques. *Journal of Climate and Applied Meteorology* 25, 1100–1124.
- Cieslik, S., Labatut, A., 1997. Ozone and heat fluxes over a mediterranean pseudosteppe. *Atmospheric Environment* 31, 177–184.
- Coe, H., Gallagher, T.W., Choularton, T.W., Dore, C., 1995. Canopy scale measurements of stomatal and cuticular O_3 uptake by Sitka Spruce. *Atmospheric Environment* 29, 1413–1423.
- Delany, A.C., Fitzjerald, D.R., Lenschow, D.H., Pearson Jr., R., Wendel, G.J., Woodruff, B., 1986. Direct measurements of nitrogen oxides and ozone fluxes over grassland. *Journal of Atmospheric Chemistry* 4, 429–444.
- Droppo Jr., J.G., 1985. Concurrent measurements of ozone dry deposition using eddy correlation and profile flux measurements. *Journal of Geophysical Research* 90, 2111–2118.
- Erisman, J.W., Pul, W.A.J., Van Wyers, P., 1994a. Parameterization of surface resistance for the quantification of atmospheric deposition of acidifying pollutants and ozone. *Atmospheric Environment* 28, 2595–2607.
- Erisman, J.W., van Elzakker, B.G., Mennen, M.G., Hogenkamp, J., Wart, E., van Den Beld, L., Römer, F.G., Bobbink, R., Heil, G., Raessen, M., Duyzer, J.H., Verhage, H., Wyers, G.P., Otjes, R.P., Möls, J.J., 1994b. The Elspeetsche veld experiment on surface exchange of trace gases: summary of results. *Atmospheric Environment* 28, 487–496.
- Fehsenfeld, F.C., Liu, S.C., 1993. Tropospheric ozone: distribution and sources. In: Hewitt, C.N., Sturges, W.T. (Eds.), *Global Atmospheric Chemical Change*, Chap. 5, Environment Management Series. Elsevier Applied Science, New York.
- Fowler, D., 1978. Dry deposition of SO_2 on Agricultural Crops. *Atmospheric Environment* 12, 369–373.
- Fuentes, J.D., Gillespie, T.J., Bunce, N.J., 1994. Effects of foliage wetness on the dry deposition of ozone onto red maple and poplar leaves. *Water, Air and Soil Pollution* 74, 189–210.
- Galbally, I.E., Roy, C.R., 1980. Destruction of ozone at the earth's surface. *Quarterly Journal of Royal Meteorological Society* 106, 599–620.
- Galbally, I.E., Miller, A.J., Hoy, R.D., Ahmet, S., Joynt, R.C., Attwood, D., 1986. Surface ozone at rural sites in the Latrobe Valley and Cape Grim, Australia. *Atmospheric Environment* 20, 2403–2422.
- Garland, J.A., 1977. The dry deposition of sulphur dioxide to land and water surfaces. *Proceedings of Royal Society of London A* 354, 245–268.
- Garratt, J.R., 1980. Surface influence upon vertical profiles in the atmosphere near surface layer. *Quarterly Journal of Royal Meteorological Society* 106, 803–819.
- Güsten, H., Heinrich, G., Schmidt, R.W.H., Schurath, U., 1992. A novel ozone sensor for direct eddy flux measurements. *Journal of Atmospheric Chemistry* 14, 73–84.
- Güsten, H., Heinrich, G., 1996a. On-line measurements of ozone surface fluxes: Part I. Methodology and Instrumentation. *Atmospheric Environment* 30, 897–909.
- Güsten, H., Heinrich, G., Mönnich, E., Sprung, D., Weppner, J., Ramadan, A.B., Ezz El-Din, M.R.M., Ahmed, D.M., Hassan, G.K.Y., 1996b. On-line measurements of ozone surface fluxes: Part II. Surface-Level ozone fluxes onto the Sahara Desert. *Atmospheric Environment* 30, 911–918.
- Hicks, B.B., Baldocchi, D.D., Meyers, T.P., Hosker Jr, R.P., Matt, D.R., 1987. A preliminary multiple resistance routine for deriving dry deposition velocities from measured quantities. *Water Air and Soil Pollution* 36, 311–330.
- Hicks, B.B., Matt, D.R., 1988. Combining biology, chemistry and meteorology in modelling and measuring dry deposition. *Journal of Atmospheric Chemistry* 6, 117–131.

- Jacobson, J.S., Hill, A.C., 1970. Recognition of Air Pollution Injury to Vegetation: a Pictorial Atlas. Air Pollution Control Association, Pittsburgh.
- Leuning, R., Unsworth, M.H., Neumann, H.N., King, K.M., 1979. Ozone fluxes to tobacco and soil under field conditions. *Atmospheric Environment* 13, 1155–1163.
- Massman, W.J., 1993. Partitioning ozone fluxes to sparse grass and soil and the inferred resistances to dry deposition. *Atmospheric Environment* 27A, 167–174.
- McMillen R.T., 1986. A basic program for eddy correlation in non-simple terrain. NOAA Technical Memorandum ERL ARL-147.
- McMillen, R.T., 1988. An eddy correlation technique with extended applicability to non-simple terrain. *Boundary-Layer Meteorology* 43, 231–245.
- Musselman, R.C., Massman, W.J., 1999. Ozone flux to vegetation and its relationship to plant response and ambient air quality standards. *Atmospheric Environment* 33, 65–73.
- Nobel, P.S., 1991. *Physicochemical and Environmental Plant Physiology*. Academic Press, United Kingdom.
- O'Dell, R.A., Taheri, M., Kabel, R.L., 1977. A model for uptake of pollutants by vegetation. *Journal Air Pollution Control Association* 27, 1104–1109.
- Padro, J., Den Hartog, G., Neumann, H.H., 1991. An Investigation of the ADOM dry deposition module using summertime O₃ measurements above a deciduous forest. *Atmospheric Environment* 25A, 1689–1704.
- Padro, J., Neumann, H.H., Den Hartog, G., 1992. Modelled and observed dry deposition velocity of O₃ above a deciduous forest in the winter. *Atmospheric Environment* 26A, 775–784.
- Padro, J., Hamilton, R.S., Revitt, D.M., Harrison, R.M., Monzon de Caceres, A., 1994a. Observed characteristics of the dry deposition velocity of O₃ and SO₂ above a wet deciduous forest. *Highway Pollution*, 395–400.
- Padro, J., Massman, W.J., Shaw, R.H., Delany, A., Oncley, S.P., 1994b. A comparison of some aerodynamic resistance methods using measurements over cotton and grass from the 1991 California Ozone Deposition Experiment. *Boundary Layer Meteorology* 71, 327–339.
- Padro, J., 1996. Summary of ozone dry deposition velocity measurements and model estimates over vineyard, cotton, grass and deciduous forest in summer. *Atmospheric Environment* 30, 2363–2369.
- Pederson, J.R., Massman, W.J., Mahrt, L., Delany, A., Oncley, S., Den Hartog, G., Neumann, H.H., Mickle, R.E., Shaw, R.H., Paw, U.K.T., Grantz, D.A., Macpherson, J.I., Desjardins, R., Schuepp, P.H., Pearson Jr, R., Arcado, T.E., 1995. California ozone deposition experiment: methods, results and opportunities. *Atmospheric Environment* 29, 3115–3132.
- Pul, W.A.J., van, 1992. The flux of ozone to a maize crop and the underlying Soil during a growing season. Ph.D. Thesis, Wageningen Agricultural University, The Netherlands.
- Rich, S., Waggoner, P.E., Tomlinson, H., 1970. Ozone uptake by bean leaves. *Science* 169, 79–80.
- Stocker, D.W., Zeller, K.F., Stedman, D.H., 1995. O₃ and NO₂ fluxes over snow measured by eddy correlation. *Atmospheric Environment* 29, 1299–1305.
- Treshow, M., Anderson, F., 1989. *Plant Stress from Air Pollution*. Wilty, Great Britain.
- Walmsley, J.L., Wesely, M.L., 1996. Modification of coded parameterisations of surface resistances to gaseous dry deposition. *Atmospheric Environment* 30, 1181–1188.
- Warneck, P., 1988. *Chemistry of the natural atmosphere*. International Geophysics Series, Vol. 41. Academic Press, London.
- Wesely, M.L., 1970. Eddy correlation measurements in the atmospheric surface layer over agricultural crops. Ph.D. Thesis, University of Wisconsin, Madison.
- Wesely, M.L., Hicks, B.B., 1977. Some factors that affect the deposition rates of sulfur dioxide and similar gases to vegetation. *Journal of Air Pollution Control Association* 27, 1110–1116.
- Wesely, M.L., Eastman, J.A., Cook, D.R., Hicks, B.B., 1978. Day time variations of ozone eddy fluxes to maize. *Boundary Layer Meteorology* 15, 361–373.
- Wesely, M.L., Eastman, J.A., Stedman, D.H., Yalvac, E.D., 1982. An eddy correlation measurement of NO₂ flux to vegetation and comparison to O₃ flux. *Atmospheric Environment* 16, 815–820.
- Wesely, M.L., 1989. Parameterisation of surface resistances to gaseous dry deposition in regional-scale numerical models. *Atmospheric Environment* 23, 1293–1304.